

# NONINTERCEPTING ELECTRON BEAM DIAGNOSTICS BASED ON OPTICAL DIFFRACTION RADIATION FOR X-RAY FELs\*

A.H. Lumpkin, W.J. Berg, N.S. Sereno, D.W. Rule<sup>†</sup>, B.X. Yang, and C.Y. Yao  
Advanced Photon Source, Argonne National Laboratory, Argonne, IL 60439 USA

## Abstract

We have successfully used near-field imaging of optical diffraction radiation (ODR) from a 7-GeV electron beam passing near a single edge of a conducting plane to obtain horizontal beam size and position information. In our experiments appreciable visible wavelength ODR is emitted for impact parameters of 1 to 2 mm, values that are close to the Lorentz factor,  $\gamma$ , times the reduced observation wavelength. An analytical model evaluated through numerical integration has been also developed. This predicts beam size sensitivity at the 20-50 micron regime for small impact parameters. Application to high-energy accelerators that drive the x-ray free-electron lasers (FELs) or energy recovering linacs (ERLs) for light sources should be possible.

## INTRODUCTION

The challenge of providing nonintercepting beam diagnostics that address transverse parameters, such as beam size and divergence, in a linear transport line continues for high-current machines that might drive x-ray free-electron lasers (FELs) [1]. We report on alternate techniques for using optical diffraction radiation (ODR) generated as a 7-GeV beam passed near a single edge of a conducting screen. The ODR mechanism has been investigated for a number of years [2-10]. For the first time we have used near-field imaging to monitor relative beam size and position along the horizontal axis, *parallel* to the edge of a vertically displaced screen [11]. In this case appreciable visible wavelength ODR is emitted for impact parameters of 1 to 2 mm, values that are close to  $\gamma\lambda \sim 1.4$  mm for  $\lambda = 0.628$   $\mu\text{m}$ . These initial experiments were done with a standard CCD camera, but we have upgraded our imaging system to include selectable bandpass filters, neutral density filters, and polarizers; a steering mirror; an optical lens setup that provides near-field or far-field imaging; and an intensified camera. Recently, a far-field experiment was reported to determine beam size [12], but this relied on the circumstance of a very low divergence beam.

We also have explored the applicability of an analytical model via numerical integration to evaluate its match to near-Gaussian transverse profiles of the ODR signal, the exponential decay of the signal with increasing impact parameter, and the modest sensitivity to beam size. We are still investigating these aspects but believe the techniques have potential for applications to x-ray FELs that are driven by multi-GeV, high-average power beams.

\*Work supported by the U.S. Department of Energy, Office of Basic Energy Sciences, under Contract No. W-31-109-ENG-38.

<sup>†</sup>Carderock Division, NSWC, West Bethesda, MD, USA 20817

## EXPERIMENTAL BACKGROUND

The Advanced Photon Source (APS) facility includes an injector complex with an rf thermionic cathode gun, an S-band linear accelerator, a particle accumulator ring (PAR) that damps the linac beam at 325 MeV, an injector synchrotron (IS) that ramps the energy from 0.325 GeV to 7 GeV in 220 ms, and the 7-GeV storage ring. At the exit of the IS, a dipole magnet allows direction of the beam to an alternate beamline (BTX) that ends with a beam dump. This spur line has been used to develop our optical transition radiation (OTR) and our ODR diagnostics. The setup includes the upstream corrector magnets, two quadrupoles, and a dipole, and then an rf beam position monitor (BPM) (vertical), the OTR/ODR imaging station, a localized beam-loss monitor based on a Cherenkov radiation detector, a Chromox beam profiling screen, and the beam dump, as schematically shown in Fig. 1.

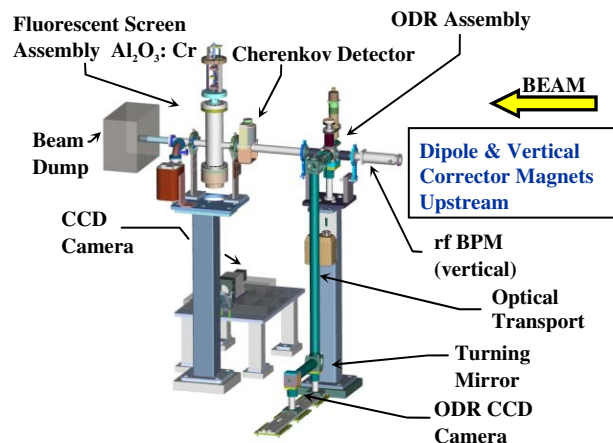


Figure 1: A schematic of the OTR/ODR test station installed in the 7-GeV BTX line at APS.

The ODR converter is a polished Al blade/mirror that is 1.5 mm thick, 30 mm wide, 30 mm tall, and it is mounted with its surface normal at 45° to the beam direction on a vertical stepper assembly. The assembly provides vertical positioning with an overall accuracy of  $\pm 10$   $\mu\text{m}$  over a span of 27.5 mm. The OTR and ODR signals were directed by turning mirrors and relay optics to a Sony visible CCD located 1.8 m from the source. The near-field magnification was chosen to cover the blade edge assembly and resulted in calibration factors of 55  $\mu\text{m}/\text{pixel}$  in  $x$  and 45  $\mu\text{m}/\text{pixel}$  in  $y$ . No bandpass filters were used in the initial experiments, but we have now added two filter wheels that allow the selection of neutral density filters, bandpass filters, or two polarizers oriented

at 90° to each other. The Pulnix-intensified CCD was recently installed, but its GaAs photocathode microchannel plate intensifier (MCP) seemed to be excessively sensitive to the ionizing radiation environment found near the beam dump. Images were obtained, but they were contaminated by the ionizing radiation events in the MCP. The Cherenkov detector was used in some of the studies to verify that the beam halo was of very limited extent at impact parameters of 4 to  $5\sigma_y$ . The ODR experiments were performed by taking five images for each blade position with an MV200 video digitizer, which provided online analysis. Gaussian functions were fit to profile distributions of the beam coming from the synchrotron as confirmed in the OTR images. The vertical beam position was monitored by the rf BPM adjacent to the ODR station and the charge by the upstream current monitor.

## ANALYTICAL BACKGROUND

A preliminary theoretical discussion of the use of ODR with a circular aperture was given in reference 8. An initial analytical model for the near-field ODR signal distribution has now been developed based on the method of virtual quanta for relativistic beams passing near a conducting plane as described by Jackson [13]. We convolved the electron beam's Gaussian distribution of sizes  $\sigma_x$  and  $\sigma_y$  with the field expected from a single electron at point  $P$  in the metal plane [11]. We wish to calculate the incoherent sum of radiation from all beam particles in a pulse emitted from a given point in the ODR radiator, i.e., at  $\mathbf{u} = \mathbf{P} - \mathbf{r}_o$ , where  $\mathbf{P}$  is the field point with respect to the origin and  $\mathbf{r}_o$  is the position of the beam centroid with respect to the origin. The impact parameter is  $\mathbf{b} = \mathbf{u} - \mathbf{r}$ , where  $\mathbf{r} = \mathbf{r}(x,y)$  denotes a position in the beam measured from the beam centroid. We can then write the differential spectral intensity as:

$$\frac{dI}{d\omega}(\mathbf{u}, \omega) = \frac{1}{\pi^2} \frac{q^2}{c} \left(\frac{c}{v}\right)^2 \alpha^2 N \frac{1}{\sqrt{2\pi\sigma_x^2}} \frac{1}{\sqrt{2\pi\sigma_y^2}} \times \iint dx dy K_1^2(\alpha b) e^{-\frac{x^2}{2\sigma_x^2}} e^{-\frac{y^2}{2\sigma_y^2}}, \quad (1)$$

where  $\omega$  = radiation frequency,  $v$  = electron velocity  $\approx c$  = speed of light,  $q$  = electron charge,  $N$  is the particle number,  $\alpha = 1/\gamma\lambda$ , and  $K_1(\alpha b) =$

$K_1\left(\alpha\sqrt{(u_x - x)^2 + (u_y - y)^2}\right)$  is a modified Bessel function. Since we measure light intensity  $I$ , this should be proportional to  $|E_x|^2 + |E_y|^2$ , resulting in the  $K_1^2$  dependence. The numerical integrations were performed and then plotted using the self-describing data set (SDDS) toolkit used at APS [14].

## RESULTS AND DISCUSSION

### Experimental Results

Examples of the OTR and ODR images are given in Fig. 2 of reference 11. We show here (Fig. 2) the Gaussian fit to an OTR image with observed beam sizes of  $\sigma_x = 1300 \pm 25 \mu\text{m}$  and  $\sigma_y = 200 \pm 25 \mu\text{m}$  for a 0.4 nC beam at 7 GeV. In Fig. 3 the Gaussian fit to the projected profile of ODR is shown for an impact parameter  $d = 1.25$  mm and  $Q = 3.4$  nC. The detected ODR horizontal image size is  $\sigma_x = 1166 \pm 50 \mu\text{m}$  about 90% of the OTR size. The blade edge distance is  $6\sigma_y$  beyond the vertical beam center but comparable to  $\gamma\lambda$ . At this  $d$ , the ODR absolute intensity is about ten times weaker than OTR, but the signal should be dominated by ODR. Our model indicates an ODR signal distribution with  $\sigma_x$  about 20% larger than the OTR beam size at  $d = 1.25$  mm, but it does not have the camera sensitivity factor included. Due to the exponential decay of ODR vertically, the signal profiles are strongest at the smaller impact parameters. We believe this behavior is characteristic of the beam dimensions, impact parameter, observation wavelength, the ODR exponential decay with impact parameter, as well as camera sensitivity effects.

The sensitivity to beam position in the horizontal axis (i.e., parallel to the blade edge) was tested by stepping the upstream dipole supply current while the blade edge was positioned about  $4\sigma_y$  above the beam center. A script using SDDS protocols was used to track the processed video image properties, the Cherenkov detector readings, and the rf BPM readings. The plot in Fig. 4 shows the horizontal ODR image centroid position versus the upstream dipole magnet supply current in A. Beam position sensitivity to about  $50 \mu\text{m}$  is seen with a slope fit of  $-0.508 \pm 0.006$  mm/A of dipole current. We expect that with a smaller inherent beam size, correspondingly smaller impact parameters, and higher optical magnification, one could approach the 10- $\mu\text{m}$  resolution regime for relative position.

The localized beam loss at the blade location was measured at the downstream Cherenkov detector [15,16] as a function of impact parameter as shown in Fig. 5. The blade step size was  $100 \mu\text{m}$ , and the signal is seen to be at the baseline at the -0.8-mm point and indistinguishable at -1.0 mm (blade above the beam in this case). The data were correlated with an SDDS toolkit option [17].

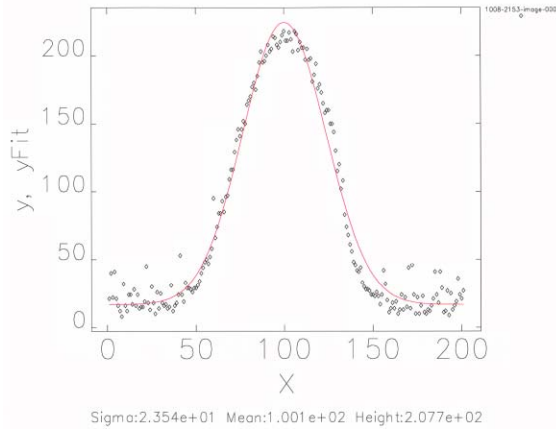


Figure 2: A plot and Gaussian fit to the OTR horizontal image profile for  $Q = 0.4$  nC and  $E = 7$  GeV.

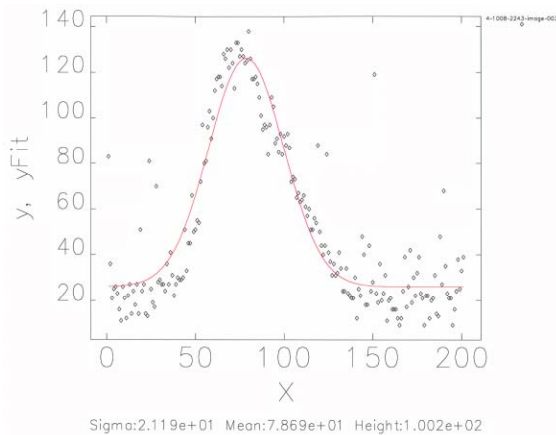


Figure 3: A plot and Gaussian fit to the ODR horizontal image projected profile with  $d = 1.25$  mm and with  $Q = 3.3$  nC and  $E = 7$  GeV.

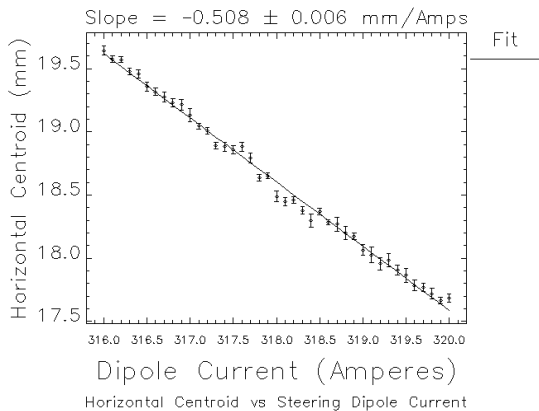


Figure 4: A plot of horizontal ODR image centroid position versus the upstream dipole magnet current supply readings. Even though the beam size is large at  $\sigma_x = 1375$   $\mu\text{m}$ , the ODR centroid shifts of  $\sim 50$   $\mu\text{m}$  are detectable.

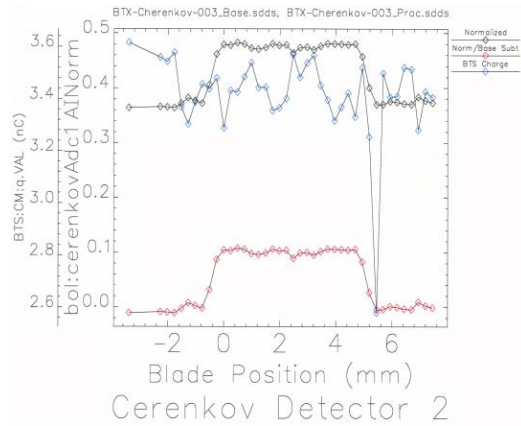


Figure 5: A plot of the localized loss monitor (Cherenkov detector) readings versus vertical blade position. The bottom plot (red) is normalized to the charge (blue) and background subtracted.

### Analytical Results

An example of the calculated ODR signal intensity 2-D spatial distribution beginning at  $d = 1.25$  mm is shown in Fig. 6. This is based on using the OTR beam sizes given in the previous subsection as input. The exponential decay of this distribution in the vertical direction is shown in Fig. 7. The decay constant is about two times that calculated from a fit of the experimental data using the  $e^{-2d/\gamma\lambda}$  function with  $\lambda = 0.85$   $\mu\text{m}$  [11]. We have not resolved this discrepancy yet.

To evaluate possible applications to smaller beam sizes, we calculated the ODR from a beam with  $\sigma_x = 20$   $\mu\text{m}$  and  $\sigma_y = 20$   $\mu\text{m}$  compared to a beam with  $\sigma_x = 50$   $\mu\text{m}$  and  $\sigma_y = 20$   $\mu\text{m}$ . For an impact parameter of  $5\sigma_y = 100$   $\mu\text{m}$ , we calculate a modest 25% difference in the profile widths as shown in Fig. 8. However, this detectable difference should allow one to monitor relative beam sizes in this regime in a high-current application, such as an x-ray FEL or ERL.

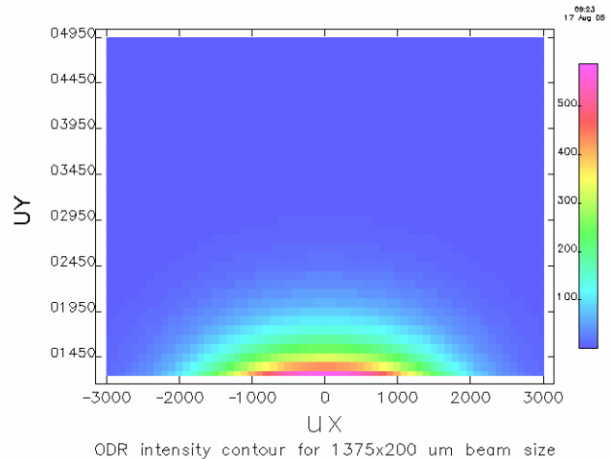


Figure 6: The calculated ODR signal distribution on the metal plane starting at  $d = 1.25$  mm for the  $\sigma_x = 1375$   $\mu\text{m}$  and  $\sigma_y = 200$   $\mu\text{m}$  case.

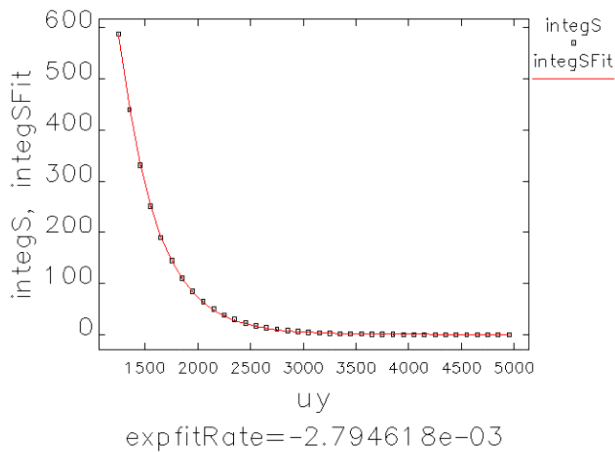


Figure 7: The plot and exponential fit of the calculated ODR y peak intensity versus impact parameter.

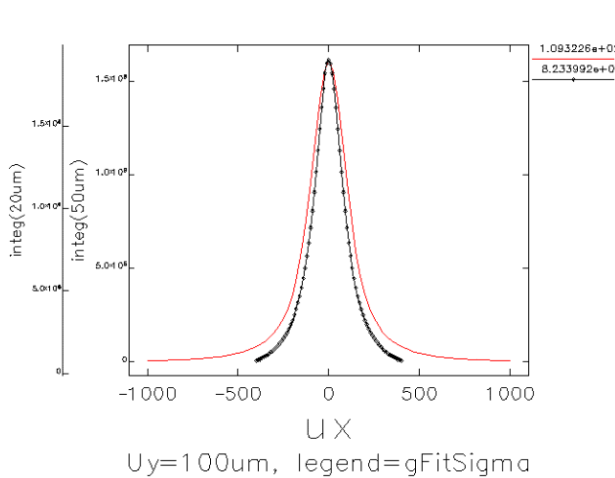


Figure 8: The comparison of the calculated ODR image horizontal profiles for  $\sigma_x = 20 \mu\text{m}$  and  $\sigma_x = 50 \mu\text{m}$  while holding  $\sigma_y = 20 \mu\text{m}$  constant. This is at the impact parameter of  $5 \sigma_y = 100 \mu\text{m}$  and shows a 25% width increase for the curve for  $\sigma_x = 50 \mu\text{m}$ .

### SUMMARY

In summary, we report our initial results, both experimental and analytical, for near-field ODR monitoring of relative beam size and position from a single-edge conducting plane. We have identified the axis parallel to the edge as the more sensitive aspect. We show that ODR has potential application to even smaller beams found in transport lines in high-energy situations, such as x-ray FELs and ERLs.

### ACKNOWLEDGMENTS

The authors acknowledge B. Rusthoven and A. Barcikowski for the mechanical design of the stepper motor and ODR blade assembly; A. Pietryla and C. Gold for the Cherenkov detector installation; L. Emery for beam loss calculations; J. Xu and S. Shoaf for controls for the ODR station and Cherenkov detector; and H. Loos (SLAC) for ODR discussions. We also acknowledge O. Singh and W. Ruzicka for project support.

### REFERENCES

- [1] Proceedings of the ICFA 17<sup>th</sup> Advanced Beam Dynamics Workshop on Future Light Sources, Argonne National Laboratory, Argonne, IL, 1999, ANL-00/8, Argonne (2000).
- [2] F.G. Bass and V.M. Yakovenko, *Sov. Phys. Uspecki* **8**(3), 420 (1965).
- [3] A.P. Kazantsev and G.I. Surdutovich, *Sov. Phys. Sokl.* **7**, 990 (1963).
- [4] M.L. Ter-Mikaelian, *High Energy Electromagnetic Processes in Condensed Media* (Wiley/Interscience, New York, 1972).
- [5] M. Castellano, *Nucl. Instrum. Methods A* **394**, 275 (1997).
- [6] Y. Shibata et al., *Phys. Rev. E* **52**, 678 (1995).
- [7] A.P. Potylitsyn, *Nucl. Instrum. Methods B* **145**, 169 (1998).
- [8] R.B. Fiorito, D.W. Rule, and W.D. Kimura, *AIP Conf. Proc.* **472**, 725 (1999); W.D. Kimura, R.B. Fiorito, and D.W. Rule, *Proc. of the 1999 Particle Accelerator Conference*, 487 (1999).
- [9] D.W. Rule, R.B. Fiorito, and W.D. Kimura, *AIP Conf. Proc.* **390**, 510 (1997).
- [10] R.B. Fiorito and D.W. Rule, *Nucl. Instrum. Methods B* **173**, 67 (2001).
- [11] A.H. Lumpkin et al., "Near-Field Imaging of Optical Diffraction Radiation Generated by a 7-GeV Electron Beam," submitted to *Phys. Rev.*, May 2005.
- [12] P. Karataev et al., *Phys. Rev. Lett.* **93**, 244802 (2004).
- [13] J.D. Jackson, *Classical Electrodynamics* (John Wiley and Sons, 1975), Sec. 15.4.
- [14] L. Emery, M. Borland, H. Shang, R. Soliday, "User's Guide for SDDS-Compliant EPICS Toolkit Version 1.5," Advanced Photon Source, March 9, 2005.
- [15] A.S. Fisher, *AIP Conf. Proc.* **451**, 95 (1998).
- [16] A. Pietryla, W. Berg, and R. Merl, 2001 Particle Accelerator Conference, Chicago, IL, 1622 (2001).
- [17] H. Shang, *Proc. of PAC2003*, 3470 (2003).